Available online at www.sciencedirect.com
SCIENCE DIRECT®
PERGAMON
International Journal of Heat and Mass Transfer 46 (2003) 2425–2444
International Journal of HEAT and MASS TRANSFER
www.elsevier.com/locate/ijhmt

Modelling and control of rectangular natural circulation loops

A. Fichera *, A. Pagano

DIIM—Università degli Studi di Catania, Viale A. Doria 6, 95125 Catania, Italy

Received 7 May 2002; received in revised form 1 November 2002

Abstract

The aim of this paper is to address the problem of suppressing unstable dynamics occurring in rectangular natural circulation loops on the base of a reliable model-based controller.

The first part of the study is devoted to define a high order model, through the reduction by truncation of the Fourier series expansion of the functions describing the loop geometry of Navier–Stokes infinite-dimensional partial differential equations describing the flow, the heating conditions and the temperature distribution of the fluid. The first three modes were considered so that a closed model of seven ordinary differential equations was obtained. The model was then integrated and simulations compared with experimental data, confirming its ability to address the description of the dynamical behaviour of rectangular natural circulation loops.

The satisfactory performances of the model lead to use it for the design and experimental testing of model-based feedback control strategies. In particular, a traditional proportional-derivative control approach has been applied to the model linearised around its equilibrium points. The flow velocity or an opportunely selected temperature difference between given points of the loop were chosen as feedback variables. Accordingly, the target of the control action was to drive the feedback variable to its stationary value, computed by means of the mathematical model. Experimental validation of the proposed model-based strategies satisfactorily demonstrated the capability of the approach in stabilising the system dynamics.

1. Introduction

Natural convection may often represent the dominant mechanism for the transfer of energy from a source to a sink, opportunely positioned with respect to one another, by means of the motion of a fluid, due to the buoyancy determined by the temperature difference between the source and the sink. Its study is eminently complex, especially in those cases characterised by high heat transfer rate, which lead to turbulent motion. Closed loop thermosyphons, also called natural circulation loops, are technical devices specifically designed in order to make use of this mechanism for the heat removal from a source, placed at bottom, to a heat sink placed at the topmost section of the loop.

As no pumps are needed, not only the cost of pumping are eliminated but also the heat removal from the heat source is intrinsically more safe. This is the main reason for preferring natural to forced convection in energy plants for which safety is a stringent requirement, as nuclear power plants and electrical machine rotor cooling [1–3], or where considerable costs reduction may be obtained, as geothermal plants and solar heaters, which are characterised by low temperature thermal source and higher circulating flow rate [4,5]. Finally, natural convection may represent one of the possible technical solution in those systems in which the pumping system cannot be conveniently positioned, such as cooling systems for internal combustion engines, turbine blade cooling or computer cooling [6,7].

Recent scientific efforts have been concentrated on two kind of geometrical configurations: the rectangular [1,8] and the toroidal [9–12]. In both cases the simplest conditions are those in which the loop lies on a vertical plane, is symmetrical with respect to the vertical axis and is made up of a bottom-placed heat source and a heat

* Corresponding author. Tel.: +39-95-7382450/337994; fax +39-95-337994.

E-mail addresses: afichera@diim.unict.it (A. Fichera), apagano@diim.unict.it (A. Pagano).

0017-9310/03/$ - see front matter © 2003 Elsevier Science Ltd. All rights reserved.
doi:10.1016/S0017-9310(02)00543-4

sink on the top. The heat source and the heat sink may be connected or not by adiabatic legs. In particular, toroidal loops reported in literature usually lack of adiabatic legs and are consist of two semicircular heat exchanging sections directly connected, whereas rectangular loops, which are the main object of the present study and are schematised in Fig. 1, usually have thermally isolated vertical legs connecting the heat exchanging sections [8]. Due to the relevance of their applications, natural circulation loops stability represents a stringent requirement. In fact, the oscillations of the fluid velocity and temperature associated to unstable dynamics are able to compromise the heat removal from the heat source and are, therefore, extremely dangerous for the plant safety. The system dynamics strongly depends both on the geometry and on the heating conditions at the boundary. It is just mentioned here that the most common heating conditions considered in literature are symmetrical and consist of: imposed wall temperature [9,11]; imposed heat flux [12–14] or mixed condition [10,15,16].

Accurate modelling of the system dynamics is necessary, so that it is possible to address the problem of its control. The geometry of the system and the heating conditions at the boundary play a fundamental role in the possibility of modelling natural circulation loops dynamics. In particular, the governing equations describing the flow inside the loop, supposed one-dimensional, have been exactly reduced to a three-dimensional dynamical model only for the case of toroidal geometry either with known wall temperature or with known heat flux. These models may display a chaotic dynamical behaviour, mainly resembling that of the Lorenz system [17]. Conversely, due to the higher complexity such simple models have not been proposed for the cases of mixed conditions or for other geometries. They lack, in particular, for the rectangular geometry with adiabatic legs as the one reported in Fig. 1, which better approximates, in general, the configuration of the most common real applications.

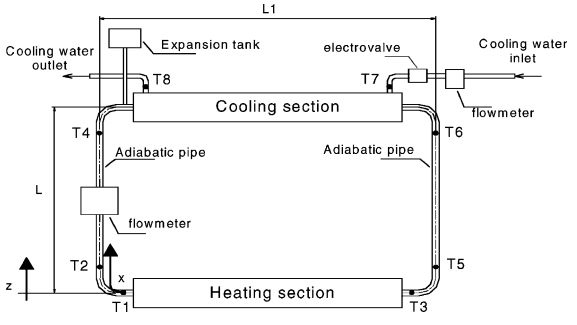

Fig. 1. Schematic of the experimental rectangular circulation loop.

The occurrence of non-periodic thermal oscillations and flow reversals in natural circulation loops represents the main problem affecting real world applications of this kind of systems. They are associated both to high local temperature and to transient stops of the fluid motion. The first phenomenon can lead to the formation of vapour bubbles able to create localised blocks to the flow, especially in those geometries characterised by small curvature bends. The second phenomenon is similar in its effects, as it leads to the momentary arrest of the heat removal from the thermal source that, depending on the application, can even represent a catastrophic event [1,2].

It is clear the opportunity to control the dynamics of natural circulation loops, aiming not only to enlarge their range of stable operations but also to guarantee reliable heat removal even during off-design transitory.

In the last ten years, starting from [9,10,18], several studies have demonstrated that one of the most attractive ways to control chaotic convective flow relies on an active feedback control strategy. Several applications based on this strategy have been proposed for the case of toroidal circulation loops and their ability in suppressing chaos has been demonstrated both in theory and in practice [19], considering either linear [18,19] or non-linear feedback [19,20]. In all reported cases, the feedback variables taken under consideration were non-dimensional temperature differences measured either at the horizontal or at the vertical diameter of the torus. These corresponded, together with the non-dimensional velocity, to the state variables of the ODE model approximating the system dynamics to the first mode. Parenthetically, the flow velocity has never been considered as feedback variable, nor it has been ever experimentally measured for control purposes.

The aims of the present study are to address the modelling of rectangular natural circulation loops and to design and testing a reliable control strategy to suppress undesired unstable dynamics. Model definition was performed by adopting the mathematical approach for generic loop geometry proposed by Rodriguez Bernal and Van Vleck [21], in order to obtain a system analogous to that describing the toroidal geometry. In particular, the model must be capable to coherently reproduce both the stationary and the chaotic flow regimes governing the system dynamics for different conditions tested on an experimental loop.

Once that the model validity was confirmed by experiments, the next step consisted in analysing, both theoretically and experimentally, the possibility to design model-based feedback control strategies, considering as feedback variables alternatively the flow velocity and the inlet–outlet temperature difference at the heating section. While the second can be considered to correspond to the horizontal temperature difference adopted in the control of toroidal loops, the flow velocity has never been

considered in simple feedback control strategies and, in general, has been considered only in the theoretical design of an optimal controller [8], which has then been experimentally tested using only temperature differences.

The design of the controller was performed in three main steps. The concern of the first was on briefly analysing the model linearised around its equilibrium points, in order to choose the correct inputs and outputs to be considered for control purposes and to assess the observability and controllability properties. The other two steps performed, respectively theoretically and experimentally, the design of traditional control strategies. In particular, the analysis was limited to the proportional and proportional-derivative control.

2. Experimental apparatus

A schematic of the experimental natural circulation loop is depicted in Fig. 1 and its main dimensions are reported in Table 1. It consists of two copper horizontal tubes (heat transfer sections), two vertical phirex tubes, four horizontal phirex tubes and four 90° phirex bends. The lower heating section consists of two independent electrical heating wire, able to provide 0.5 kW each, winding on the outside of the copper tube.

The upper heat extraction system is a coaxial heat exchanger with tap water flowing in the annulus created by an external iron case (diameter 0.2 m). An expansion tank open to the atmosphere is installed on the topmost elevation of the loop allowing the fluid volumetric expansion.

The whole system is equipped with six calibrated (precision ±0.1 K) T-thermocouples (diameter 0.5 mm) located (refer to Fig. 1): T2 and T4 on the left vertical tube, T5 and T6 on the right vertical tube and T1 and T3 on the lower horizontal tubes. Moreover, a magnetic flow meter model MAG MASTER—ABB, which does not interfere with the flow, is placed in the middle of one of the vertical legs and measures the mass flow rate circulating in the loop (error on the velocity ±0.00075 m/s).

Hence, the result of each experimental test consists of seven time series describing the dynamical behaviour of the temperatures measured along the loop and of the mass flow rate. The temperatures are indicated in the following with the same name of the thermocouples they are measured with.

The thermocouples and the flow meter are connected to a National Instruments board, model 6052E, connected to a SCXI 1102. During each test and for each measurement, the acquisition board stores 5 data per second in a buffer and then records the mean value of these 5 data; this in practice results in a sampling period of 1 s that allows the suppression of high frequency noise components.

Table 1
Main dimensions of the experimental loop

	Loop main dimensions [mm]
Loop height	680
Loop width	1450
Tube inner diameter	26
Heating section length	930
Cooling section length	1000
Total loop length	5260

3. Mathematical model

This section addresses the mathematical modelling of the dynamical behaviour of the rectangular natural circulation loop schematised in Fig. 1. The system is characterised by having generic height and width, indicated respectively with L and L_1, and constant tubes inner diameter, r. In the following, x represents an abscissa parallel to the loop pipes with positive direction corresponding to the clockwise path on the loop and arbitrarily chosen origin in the left down corner of the loop. Writing the equation of mass conservation, in the hypotheses of uncompressible fluid and of one-dimensional motion, implies that the cross-section averaged flow velocity is the same at all points along the loop and hence $\omega = \omega(t)$, which ensures that the velocity field does not depend on the abscissa x.

The balance of the forces acting on the elementary piece of tube of length dx yields:

$$\rho\pi r^2 \cdot \mathrm{d}x \cdot \frac{\mathrm{d}\omega(t)}{\mathrm{d}t} = -\pi r^2 \cdot \mathrm{d}x \cdot \frac{\mathrm{d}p}{\mathrm{d}x} - \rho g \cdot \pi r^2 \cdot \mathrm{d}x \cdot \frac{\mathrm{d}z}{\mathrm{d}t} - \tau_w \cdot 2\pi r \cdot \mathrm{d}x \tag{1}$$

Under Boussinesq assumption, it is possible to neglect the variation of density with temperature everywhere except that in the buoyancy term, where a linear dependence on temperature can be assumed. Let T_0, T, $\rho_0 = \rho(T_0)$ and β denote respectively the reference temperature, the fluid temperature at the generic abscissa, the reference density and the volumetric expansion coefficient (supposed constant for simplicity). Hence, Boussinesq's hypothesis reads $\rho = \rho_0[1 - \beta(T - T_0)]$; substituting in (1), dividing for $\pi r^2\,\mathrm{d}x$ and integrating over the whole length of the loop leads to

$$\rho_0 \frac{\mathrm{d}\omega(t)}{\mathrm{d}t} = \frac{\rho_0 g \beta}{2(L + L_1)} \oint (T - T_0) f(x)\,\mathrm{d}x - \frac{2\tau_w}{r} \tag{2}$$

In the previous equations the function $f(x)$ is used to describe the loop geometry through the variation in height of the abscissa x, i.e. $f(x) = \mathrm{d}z/\mathrm{d}x$. Referring to Fig. 1, $f(x)$ is a piecewise function that assumes the following discrete values (refer to Fig. 2(a)):

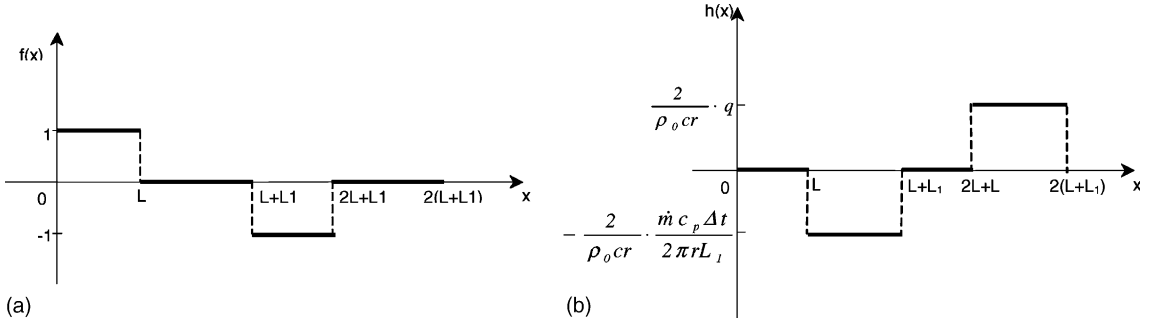

Fig. 2. Piecewise linear functions describing: (a) the loop geometry, (b) the heating boundary conditions.

$$f(x)=\begin{cases}1 & 0<x<L\\ 0 & L<x<L+L_1\\ -1 & L+L_1<x<2L+L_1\\ 0 & 2L+L_1<x<2(L+L_1)\end{cases} \tag{3}$$

which for a closed loop implies $\oint f(x)=0$.

In accordance with [14] and [16], the term τ_w can be expressed as

$$\tau_w=\frac{1}{2}\rho_0 f^*\omega^2 \tag{4}$$

where

$$f^*=\frac{b}{Re^d}\quad Re=\frac{\rho_0 v 2r}{\mu}=\frac{\omega 2r}{\nu} \tag{5}$$

where μ and ν denote the dynamic and cinematic viscosity respectively, which have been considered constant and independent on temperature. The validity of this assumption might be limited by the existence of high temperature oscillations; nonetheless, further complication of the model is out of the scope of this study. Substituting (5) in (4)

$$\tau_w=\frac{1}{2}\rho_0 b\left(\frac{\nu}{2r}\right)^d\omega^{2-d} \tag{6}$$

The momentum equation is therefore

$$\frac{\mathrm{d}\omega(t)}{\mathrm{d}t}+\frac{1}{r}b\left(\frac{\nu}{2r}\right)^d\omega^{2-d}=\frac{g\beta}{2(L+L_1)}\oint(T-T_0)f(x)\,\mathrm{d}x \tag{7}$$

In order to assess of the energy balance equation it is necessary to choose the thermal conditions at the loop walls. In particular, the vertical legs, for $0<x<L$ and $L+L_1<x<2L+L_1$, are supposed adiabatic; in the horizontal bottom section, of length L_1, it has been assumed a constant heat flux q, uniformly distributed per unit length; at the horizontal top section, i.e. at the heat exchanger of length L_1, the fluid circulating inside the loop is cooled by the fluid circulating in the outer cylinder of the heat exchanger.

A strong assumption has been considered in the following, in order to allow an exact closed form reduction of the mathematical model. In particular, as no exact reduction is possible if mixed heating conditions are considered and as it has been assumed a uniformly distributed heating flux at the bottom section, an analogous and opposite cooling flux has been assumed at the topmost horizontal section. In practice, under this hypothesis if ΔT is the inlet–outlet temperature difference of the external cooling flow rate, the heat extracted in an elementary area is $\dot m c_p\Delta T/2\pi r L_1$, with $\dot m$ and c_p the mass flow rate and specific heat of the cooling fluid. Notice that, the last condition is hardly feasible in real applications as it requires an uniform heat extraction over the length of the tube; hence, a posteriori comparisons of experimental results and model simulations ought to confirm the validity of the model. Parenthetically, similar mismatches between the boundary conditions chosen for the model and allowing simple closed reduction and those used during experiments to test the model itself have been considered in analogous cases by many authors [9,10,22,23]. With the aforementioned heating boundary conditions, the energy balance of the control volume of length dx, can be expressed as

$$\frac{\partial T}{\partial t}+\omega(t)\frac{\partial T}{\partial x}=h(x)+a\frac{\partial^2 T}{\partial x^2} \tag{8}$$

where for simplicity, the boundary conditions have been expressed in compact form through the piecewise function $h(x)$ (see Fig. 2 (b)):

$$h(x)=\begin{cases}0 & 0<x<L\\ -\frac{2}{\rho_0 cr}\cdot\frac{\dot m c_p\Delta t}{2\pi r L_1} & L<x<L+L_1\\ 0 & L+L_1<x<2L+L_1\\ \frac{2}{\rho_0 cr}\cdot q & 2L+L_1<x<2(L+L_1)\end{cases} \tag{9}$$

Summarising, the mass, momentum and energy balance equations, with geometry, boundary conditions and shear stress coefficient expressed by the functions $f(x)$, $h(x)$ and τ_w respectively, constitute the mathematical model of the generic natural circulation loop, which reads

$$\frac{\mathrm{d}\omega(t)}{\mathrm{d}t}+\frac{1}{r}b\left(\frac{v}{2r}\right)^{d}\omega^{2-d}=\frac{g\beta}{2(L+L_1)}\oint(T-T_0)f(x)\,\mathrm{d}x;\quad \omega(0)=\omega_0 \tag{10}$$

$$\frac{\partial T}{\partial t}+\omega(t)\frac{\partial T}{\partial x}=h(x)+a\frac{\partial^2 T}{\partial x^2};\quad T(x,0)=T_0(x) \tag{11}$$

It is possible to see that the model is formed by a one-dimensional ordinary differential equation and an infinite-dimensional partial differential equation. In order to obtain a finite order model, which can therefore be applied for the study of the system dynamics or for its simulation, it is necessary to find a way to reduce the infinite-dimensional model (10) and (11) to a finite-dimensional one.

3.1. Model reduction

Rodriguez-Bernal and Van Vleck [21] described the way to reduce a model formally identical to (10) and (11), by means of the following Fourier series expansion of the known functions $f(x)$ and $h(x)$ and of the variable $T(x,t)$:

$$T(x,t)-T_0=\sum_{k\in Z^*}a_k(t)\cdot \mathrm{e}^{\mathrm{i}\frac{2\pi}{2(L+L_1)}kx} \tag{12}$$

$$h(x)=\sum_{k\in K}b_k\cdot \mathrm{e}^{\mathrm{i}\frac{2\pi}{2(L+L_1)}kx} \tag{13}$$

$$f(x)=\sum_{k\in J}c_k\cdot \mathrm{e}^{\mathrm{i}\frac{2\pi}{2(L+L_1)}kx} \tag{14}$$

where $K,J\subset Z^*=Z\setminus\{0\}$. The substitution of (12)–(14) in (10) and (11) leads to the following infinite system of ordinary differential equations:

$$\frac{\mathrm{d}\omega(t)}{\mathrm{d}t}+\frac{1}{r}b\left(\frac{v}{2r}\right)^{d}\omega^{2-d}=g\beta\sum_{k\in K\cap J}a_k(t)\cdot\bar{c}_k \tag{15}$$

$$\frac{\mathrm{d}a_k(t)}{\mathrm{d}t}+\left[\frac{\pi}{(L+L_1)}\mathrm{i}k\omega(t)+a\frac{\pi^2}{(L+L_1)^2}k^2\right]\cdot a_k(t)=b_k \quad \text{with } k\subset K\cap J \tag{16}$$

in which $\bar{a}_k(t)=a_{-k}(t)$; $\bar{b}_k=b_{-k}$; $\bar{c}_k=c_{-k}$.

In the case of rectangular loops herein considered, the coefficients c_k of the Fourier expansion of $f(x)$ result from the following equation:

$$c_k=\frac{1}{2(L+L_1)}\oint f(x)\cdot \mathrm{e}^{-\mathrm{i}\frac{2\pi}{2(L+L_1)}kx}\,\mathrm{d}x \tag{17}$$

Substituting for simplicity the following expressions and considering (7):

$$\vartheta=\frac{\pi x}{L+L_1}\quad \gamma=\frac{\pi L}{L+L_1} \tag{18}$$

the coefficients c_k for the rectangular geometry become

$$c_k=\frac{1}{2\pi k\mathrm{i}}[(1-\cos k\gamma+\mathrm{i}\sin k\gamma)(1-\cos k\pi)] \tag{19}$$

that vanish for even k.

Acting analogously for the calculation of the coefficient b_k of the expansion of $h(x)$, considering (9), yields

$$b_k=\frac{1}{2(L+L_1)}\oint h(x)\cdot \mathrm{e}^{-\mathrm{i}\frac{2\pi}{2(L+L_1)}kx}\,\mathrm{d}x \tag{20}$$

Substituting again (18) and the following:

$$\Gamma=\frac{2}{\rho_0 cr}\left(\frac{\dot{m}c_p\Delta T}{2\pi rL_1}+q\right)\quad \Gamma_1=\frac{2}{\rho_0 cr}\left(\frac{\dot{m}c_p\Delta T}{2\pi rL_1}-q\right) \tag{21}$$

the coefficient b_k read

$$b_k=\frac{\Gamma}{2\pi k\mathrm{i}}(-1-\cos k\gamma+\mathrm{i}\sin k\gamma)\quad \text{for odd } k \tag{22}$$

$$b_k=\frac{\Gamma_1}{2\pi k\mathrm{i}}(1-\cos k\gamma+\mathrm{i}\sin k\gamma)\quad \text{for even } k \tag{23}$$

The a_k of the expansion of $T(x,t)$ are complex and can be expressed as

$$a_k(t)=\alpha_k(t)+\mathrm{i}\beta_k(t) \tag{24}$$

In order to obtain a finite model it is necessary to approximate the Fourier series expansion to a finite number of modes. In the present study the first three modes ($k=3$) have been considered sufficient, according to the following considerations:

- the first mode of the series expansions of $f(x)$ and $h(x)$ is sinusoidal; therefore, it is unable to approximate the original square wave-shapes functions;
- the second mode of the series expansion of $f(x)$ according to Eq. (19) is null and therefore does not contribute to the regime dynamical behaviour;
- numerical simulations have shown that the dynamical contribute of the third mode, though much smaller than the first and more strongly damped, is still relevant to reach an adequate approximation of the system dynamics;
- simulations of the fifth mode have shown that its contribution is negligible; moreover frequencies associated to this mode (and to the higher order modes) can be considered out of the range of frequencies that is interesting to model in practice.

Application of the method of residuals to Eqs. (15) and (16), in order to separate the terms of the same order, substitution of a_i, b_i, and c_i and separation of real and imaginary parts, leads to yields:

$$\dot{\omega}(t) = -\frac{1}{r} b \left(\frac{v}{2r}\right)^d \omega^{2-d} + \frac{2g\beta}{\pi}\left[\alpha_1(t)\sin\gamma - \beta_1(t)(1-\cos\gamma) + \alpha_3(t)\frac{1}{3}\sin 3\gamma - \beta_3(t)\frac{1}{3}(1-\cos 3\gamma)\right] \tag{25}$$

$$\dot{\alpha}_1(t) = -a\frac{\pi^2}{(L+L_1)^2}\alpha_1(t) + \frac{\pi}{L+L_1}\omega(t)\beta_1(t) + \frac{\Gamma}{2\pi}\sin\gamma \tag{26}$$

$$\dot{\beta}_1(t) = -a\frac{\pi^2}{(L+L_1)^2}\beta_1(t) - \frac{\pi}{L+L_1}\omega(t)\alpha_1(t) + \frac{\Gamma}{2\pi}(1+\cos\gamma) \tag{27}$$

$$\dot{\alpha}_2(t) = -a\frac{4\pi^2}{(L+L_1)^2}\alpha_2(t) + \frac{2\pi}{L+L_1}\omega(t)\beta_2(t) + \frac{\Gamma_1}{4\pi}\sin 2\gamma \tag{28}$$

$$\dot{\beta}_2(t) = -a\frac{4\pi^2}{(L+L_1)^2}\beta_2(t) - \frac{2\pi}{L+L_1}\omega(t)\alpha_2(t) - \frac{\Gamma_1}{4\pi}(1-\cos 2\gamma) \tag{29}$$

$$\dot{\alpha}_3(t) = -a\frac{9\pi^2}{(L+L_1)^2}\alpha_3(t) + \frac{3\pi}{L+L_1}\omega(t)\beta_3(t) + \frac{\Gamma}{6\pi}\sin 3\gamma \tag{30}$$

$$\dot{\beta}_3(t) = -a\frac{9\pi^2}{(L+L_1)^2}\beta_3(t) - \frac{3\pi}{L+L_1}\omega(t)\alpha_3(t) + \frac{\Gamma}{6\pi}(1+\cos 3\gamma) \tag{31}$$

One main consideration must be drawn at this point. Considering the system dynamics at regime, it is necessary that the global heat power supplied to the fluid in the heat source is then extracted in the heat sink, in order to have a non-diverging thermal field. This leads to consider for the regime condition:

$$\oint h(x) = 0 \tag{32}$$

which together with (9) and (21) implies that $q = -(\dot{m}c_p\Delta t/2\pi r L_1)$ and $\Gamma_1 = 0$.

It is important to notice that, the last observation leads to the non-controllability of the second mode, expressed by Eqs. (28) and (29), which is, on the other hand, stable and rapidly decaying. Anyhow, system (25)–(31) represents the mathematical model, approximated to the third order, of the dynamics of rectangular natural circulation loops.

Once that the model has been simulated it is necessary to rebuild the temperature dynamics $T(x,t)$ from the simulated variables $\alpha_k(t)$ and $\beta_k(t)$, i.e. real and imaginary part of the expansion coefficients of $T(x,t)$. This is easily performed according to (12), arresting the sum at the third mode:

$$\begin{aligned} T(x,t) - T_0 = {} & 2\alpha_1(t)\cos\frac{\pi}{L+L_1}x - 2\beta_1(t)\sin\frac{\pi}{L+L_1}x \\ & + 2\alpha_2(t)\cos\frac{\pi}{L+L_1}2x - 2\beta_2(t)\sin\frac{\pi}{L+L_1}2x \\ & + 2\alpha_3(t)\cos\frac{\pi}{L+L_1}3x - 2\beta_3(t)\sin\frac{\pi}{L+L_1}3x \end{aligned} \tag{33}$$

3.2. Model validation

In order to validate the model it is necessary to compare its simulation with the measurements detected on the experimental loop described in the second section. The parameters that have been adopted during the simulations are reported in Table 2.

They correspond to the fluid properties at the reference temperature $T_0 = 55$ °C and can be considered constant. The other parameters, a, b and d, are strongly dependent on the fluid motion which occurs during the various operating condition. Those used in this study are reported in Table 3.

Some explanations are needed to justify previous choices. The experimental determination of parameters a, b and d is quite uncertain and this cause the existence of strong differences between the values reported by various authors, as described in [16]. For this reason, the values that we have reported represent just an attempt to fit simulated with experimental data. Some physical reasoning of the relevant changes existing for different power level can nonetheless be given:

- For heat power below 900 W, the flow it stationary and therefore it has a constant non-zero flow velocity. The value of the thermal diffusivity that has been found derives mainly from the turbulent component due to the constant stationary velocity.
- For heat power between 900 and 1600 W, the flow is not stationary but chaotic. The kind of chaotic motion that the experimental system manifests is the so called one-side chaos (see the left column of Fig. 5),

Table 2
Fluid properties

β	5.040×10^{-4} K^{-1}
ρ	985.73 kg m^{-3}
c_p	4.183 kJ kg^{-1} K^{-1}
v	0.5×10^{-6} m^2 s^{-1}

Table 3
Dissipative terms

Power	a [m^2 s^{-1}]	b [1]	d [1]
<900 W	0.004	2	0.5
900–1600 W	0.0002	36	0.9
>1600 W	0.0002	2	0.5

described in [24]. This means that the flow velocity oscillates mainly in the positive half-plane, from values around zero (with very weak and brief flow reversals) to a variable maximum. In practice, there is a sort of fluctuation between laminar and turbulent flow, occurring when the velocity is around respectively zero and the maximum. This justifies the reduction of parameter a and the increase of b and d.

- For heat power over 1600 W, the system is still chaotic but with a "two-sides" attractor (see the right column of Fig. 5). This means that in the average the system spends less time in the region around the zero flow velocity. This has lead to parameters b and d equal to the first range of heat powers (corresponding to a dominance of turbulent motion) but parameter a equal to that of the second range of heat powers (which accounts for the influence of the low velocity region around flow reversal).

Various experimental tests have been performed in order to validate the mathematical model. Preliminary analyses of the experimental data have shown that the onset of unstable dynamics occurs for heat power ranging around 1000 and 1100 W. Over this heat power the flow is always unstable whereas below this value it is stable, unless rapid perturbation increases the heat power supply more than about 150 W.

For the sake of model validation, here are reported just the experimental conditions characterised by heat power values of 800, 1500 and 2200 W, as they well represent the possible dynamics of the system.

Due to the chaotic behaviour of the system in study, the comparisons between experimental and simulated data have been performed only on the basis of a qualitative approach, analogously to what has been proposed elsewhere [9]. In fact, a direct comparison of time series coming from systems (or models) that are not identical is impossible due to the strong dependence on initial conditions typical of chaotic motion [25,26]. This problem cannot be solved, as in a real system measurement uncertainties and noise are always present. Therefore, the comparison has been limited to verify the existence of morphological similarities between experimental and simulated time series and between their attractors in phase space. The comparison in the time domain implies that the experimental and simulated time series can be considered in good accordance if their waveforms, as well as their mean values, their frequencies and their oscillation ranges, are approximately similar. In phase space it has been considered sufficient to verify the existence of morphological similarities between the experimental and simulated attractors.

Fig. 3 reports the comparisons of the experimental (left column) and simulated (right column) time series $\Delta T25 = T2 - T5$ for a heat power supplied to the heat exchanger of 800 W. Apart from the relevant amount of noise in the experimental data, which is anyway peculiar of the stationary conditions, the ability of the model to reproduce the system dynamics for low heat power supply is clear, both for the overall transient behaviour and for the stationary value reached after it. Parenthetically, the flow inversion that occurs in the simulation is simply due to the casual choice of the initial conditions.

For higher heat power values the system dynamics does not converge to a stationary solution and may be characterised by different kinds of oscillations. Fig. 4 reports the comparisons for experimental and simulated time series $\Delta T25 = T2 - T5$; the left and right columns report the plots for a heat power supplied to the heat exchanger respectively of 1500 and 2100 W. These plots give a clear indication of the capability of the model of reproducing the dynamical behaviour of the experimental rectangular natural circulation loop. In fact, there is sufficient evidence that the waveforms characterising the experimental time series are analogous to those describing the simulated time series.

Also, the amplitude and frequencies characterising the system and the model are in the overall comparable. The analysis of the plots also shows the capability of the model in reproducing with satisfying accuracy the two main dynamical case of the system in study. The model simulates satisfactorily the operating conditions with negligible flow reversals, as it happens for relatively low heat power (e.g. 1500 W), whit oscillations mainly maintaining the same sign. This behaviour has been

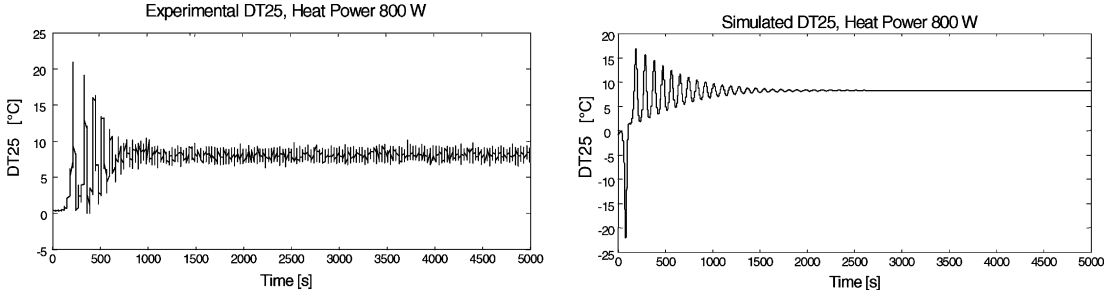

Fig. 3. Comparison of the experimental and simulated time series of temperature difference $\Delta T25 = T2 - T5$ for $P = 800$ W.

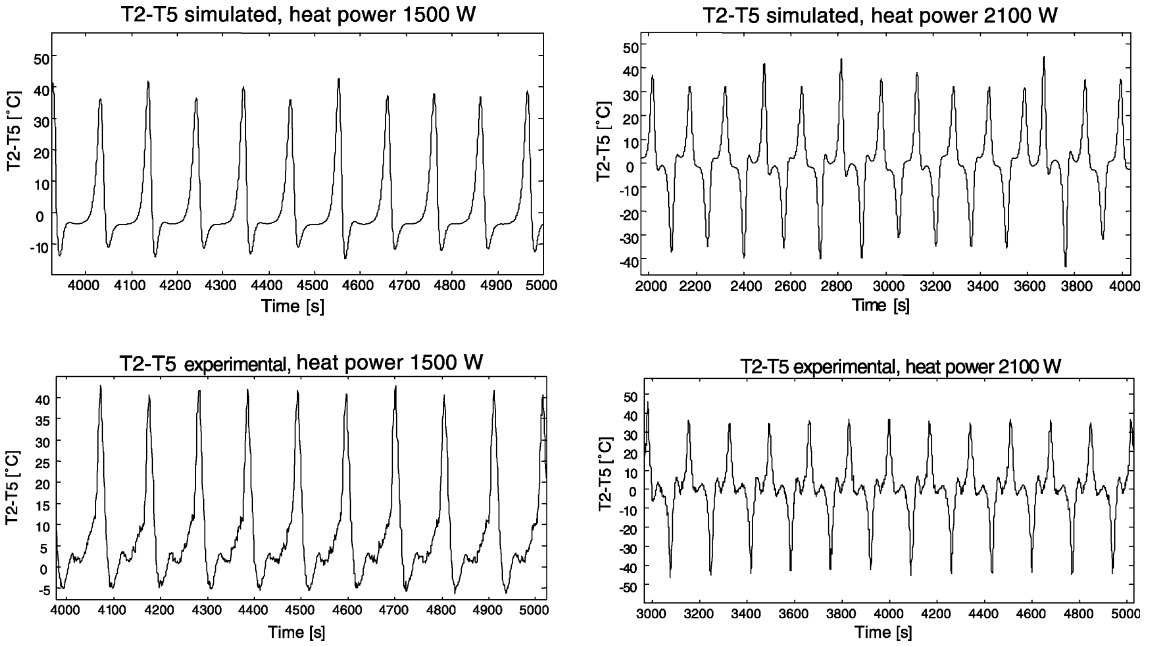

Fig. 4. Comparison of the experimental and simulated time series of temperature difference $\Delta T25 = T2 - T5$ for heat power: $P = 1500$ W (first column), $P = 2100$ W (second column).

experimentally found to happen in both directions, the sign of oscillations primarily depending on the initial conditions. The model is also capable of simulating operating conditions with well-developed flow reversals, for which the temperature difference frequently change sign, as it happens for the heat power 2100 W. The comparisons concerning the velocity follow the same patterns of those on temperature difference and, therefore, have not been reported.

Fig. 5 reports the comparison in phase space for the same cases described in Fig. 4. The left and right columns report the attractors for heat power 1500 and 2100 W respectively. Reminding that it is possible to draw just qualitative consideration on the similarity existing between the experimental (first row) and simulated (second row) attractors, the comparison, once again, confirms the satisfactory performance of the model in the description of the system dynamics. In fact, it is evident how striking the simulated attractors resemble those describing the experimental dynamics. Moreover, the satisfactory performances of the model indirectly prove also the validity of the assumption made on the heating boundary conditions, where a constant and uniform heat extraction at the cooling section was considered in order to allow the model reduction.

3.3. Preliminary analysis of the model

The design of the controller moved from the mathematical model described in the previous sections. The first step towards the design of a controller consists in calculating the stationary points of the model and in analysing their stability. In practice the control action will aim to ensure the stability of the stationary solutions during operations for which they are unstable in the uncontrolled flow. These points are obtained from model (25)–(31) annulling the time derivatives of the state variables and solving the resulting set of algebraic equations. Three stationary points are found in this way. Two points are symmetric, as a consequence of the geometrical symmetry of the loop, and correspond to the stationary motion that may occur with equal probability either in the clockwise or in the counter-clockwise direction; they will be referred in the following as $SP1$ and $SP2$. The third point, $SP3$ in the following, corresponds to the absence of motion; in practice this case is possible only when no geometrical or thermal perturbations alter the ideal symmetry of the system, and is characterised by the transfer of heat from the source to the sink only through the conduction mechanism, i.e. without convection. Due to the weakness of conductive heat transfer, $SP3$ is usually highly unstable. In practice it is stable only for very low values of the heat power.

In order to analyse the stability of the system, the model has been linearised around the equilibrium points, determining the jacobian matrix and studying its eigenvalues, and observability and controllability of the linearised model have been characterised.

Referring to the symmetric equilibrium points $SP1$ and $SP2$, which are those of interest for practical appli-

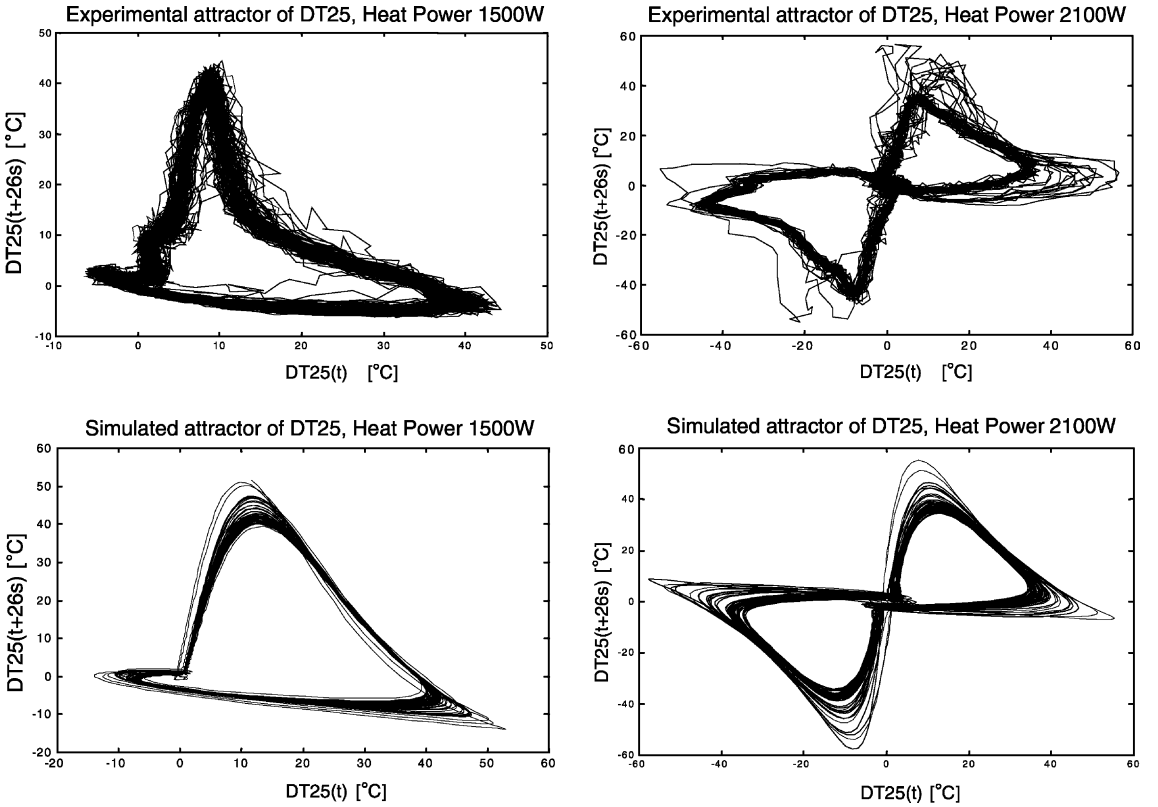

Fig. 5. Comparison of experimental and simulated attractors of $\Delta T25 = T2 - T5$, for heat power: $P = 1500$ W (left column), $P = 2100$ W (right column).

cations, it has been found that the linearised model around this equilibria is completely observable but not controllable. In particular, the subset describing the second mode (Eqs. (28) and (29)) does not depend directly on variations of the heat power, on which the control action can be exerted. Nonetheless, this non-controllable subsystem is stable and therefore the global linearised system is stabilisable. This has been confirmed also by a wide set of simulations of the non-linear system, for which convergence to zero of the second mode has been always observed. In practice, for the purpose of control, it has been verified that the uncontrollability of the second mode does not pose a problem.

It is interesting to underline that the stability of the second non-controllable mode is guaranteed by the absence of forcing therefore as well as by the thermal damping associated to the thermal diffusivity a. This is an important point that confirms the choice made at the beginning of this study, in accordance with the suggestion reported in [21], of taking into account also the thermal diffusivity. In fact, higher order models for natural circulation loops, at least for the case of rectangular geometry, cannot neglect the terms depending on thermal diffusion, on the contrary of what is commonly done for toroidal thermosyphons, reducing their dynamics to the first mode [10,18–20].

The analysis of the poles of the linearised systems for solutions $SP1$ and $SP2$ has been performed gradually increasing the heat power. These points are stable for low heat power values (up to 1100 W) and unstable for greater values, which agrees with the onset of unstable dynamics found during the experiments.

Fig. 6 shows the maximum real part of the eigenvalues of the linearised model with respect to the heat

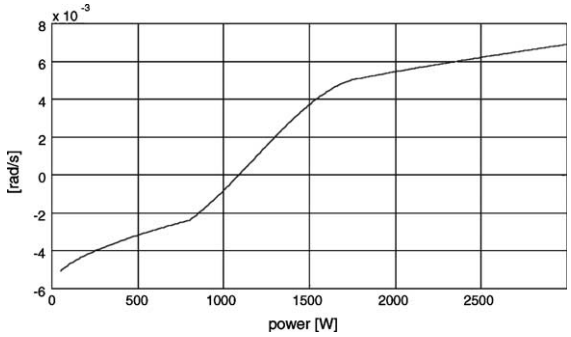

Fig. 6. Maximum real part of the eigenvalues of the linearised model.

power. Notice that the particular (non-parabolic) shape of this plot is simply due to the variations of the parameters of the model, as reported in Tables 2 and 3.

4. Controller design

The main purpose of the control action is to avoid temperature and velocity oscillations in the loop, which compromise efficient heat removal from the heat source. From now on, the study has been focused on the design of controllers aiming to stabilise solutions $SP1$ and $SP2$, in particular to the first of them, which is associated to the clockwise motion of the fluid and hence, with the convention adopted, to the positive stationary velocity. The problem of stabilising $SP3$ has been neglected as it is out of the scope of the present paper.

The equilibrium conditions have been derived from the model for a set of given nominal values of the heat power and all the controllers have been designed to provide deviations around this power.

Several controllers have been designed on the base of the linearised model and then tested both on a simulator of the non-linear ODE model and on the real system. The differences between the controllers regard the choice of the feedback variable and of the control law.

In particular, temperature difference $\Delta T25 = T2 - T5$ (i.e. the inlet–outlet temperature difference at the heating section, indicated in the previous section as ΔT_{hs}) or the fluid velocity have been adopted as feedback variables.

The first choice that has been considered in this study has been the design of a feedback controller with proportional action, aiming to shift the real part of the poles of the system from positive to negative values. The general well-known scheme for the generic output of the system (or of the model), Y, is reported in Fig. 7(a), evidencing that the nominal input U_{nom} is modified by a term proportional, through the gain K_p, to the difference existing between the actual and the reference system output.

Considering as reference output the stationary values of the feedback variable for the given input, the only unknown in the scheme is the gain K_p that ensures the stability of the controlled system with the desired rapidity of convergence to the desired stationary solution.

The next step in the direction of the design of the controller is represented by the optimisation of the performance of the controller. In particular, the simple proportional strategy, though it may be able to suppress the unstable dynamics and to drive the system to the desired stationary solution, may nonetheless suffer of relevant oscillations of both the feedback and the control variable and of excessively long transient. As well known, both these problems can be solved by adding a derivative action to the proportional term. This new term increases the global control action proportionally to the derivative of the difference between the actual and the reference value of the feedback variable, as reported in Fig. 7(b). In this way it is possible to anticipate the action of the controller, smoothing it and reducing both the amplitude of the oscillations of the controlled system and the transient.

In all the experiments and the simulations the control action has been turned on after that the system had manifested a sufficiently developed oscillating behaviour, in order to show the capability of the controllers both in maintaining the system stability and in stabilising its dynamics starting from unstable conditions.

4.1. Proportional and proportional-derivative control on velocity

From a mathematical point of view, the flow velocity, ω, is the only real variable directly simulated by the model and its value can be measured in any point of the loop, as a direct consequence of the assumption of uncompressible fluid. Therefore, the simplest controller is obtained considering the proportional strategy for the suppression of the oscillations of the velocity around its stationary value.

This assumption leads to modify the mathematical model describing the free dynamics of the system, by addition of the control term $K_{pv}(\omega_{\mathrm{ref}} - \omega)$ to those terms that contain the input Γ, which must be modified accordingly as

$$\Gamma = \Gamma_{\mathrm{nom}} + K_{p\omega}(\omega_{\mathrm{ref}} - \omega) + K_{d\omega}\dot{\omega} \tag{34}$$

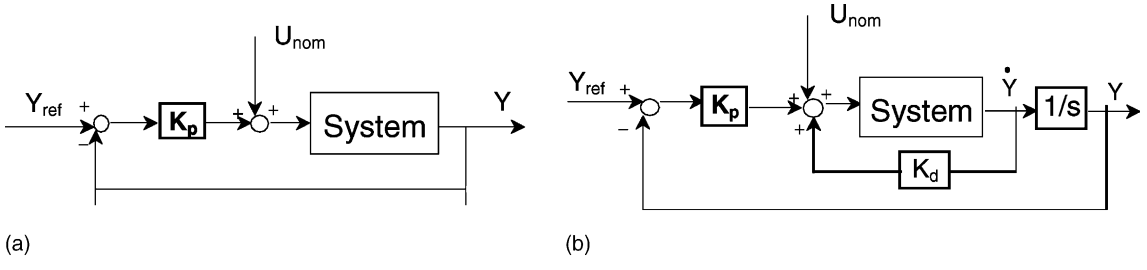

Fig. 7. Proportional (a) and proportional-derivative (b) feedback control scheme for the generic system output Y.

In this way the equations of the model for the controlled system become:

$$\begin{aligned}
\dot{\omega}(t) &= -\frac{1}{r}b\left(\frac{v}{2r}\right)^{d}\omega^{2-d} + \frac{2g\beta}{\pi}\left[\alpha_1(t)\sin\gamma - \beta_1(t)\right. \\
&\quad \left.\times(1-\cos\gamma) + \alpha_3(t)\frac{1}{3}\sin 3\gamma - \beta_3(t)\frac{1}{3}(1-\cos 3\gamma)\right] \\
\dot{\alpha}_1(t) &= -a\frac{\pi^2}{(L+L_1)^2}\alpha_1(t) + \frac{\pi}{L+L_1}\omega(t)\beta_1(t) \\
&\quad + \frac{\sin\gamma}{2\pi}\left[\Gamma_{\text{nom}} + K_{p\omega}(\omega_{\text{ref}}-\omega) + K_{d\omega}\dot{\omega}\right] \\
\dot{\beta}_1(t) &= -a\frac{\pi^2}{(L+L_1)^2}\beta_1(t) - \frac{\pi}{L+L_1}\omega(t)\alpha_1(t) \\
&\quad + \frac{(1+\cos\gamma)}{2\pi}\left[\Gamma_{\text{nom}} + K_{p\omega}(\omega_{\text{ref}}-\omega) + K_{d\omega}\dot{\omega}\right] \\
\dot{\alpha}_2(t) &= -a\frac{4\pi^2}{(L+L_1)^2}\alpha_2(t) + \frac{2\pi}{L+L_1}\omega(t)\beta_2(t) + \frac{\Gamma_1}{4\pi}\sin 2\gamma \\
\dot{\beta}_2(t) &= -a\frac{4\pi^2}{(L+L_1)^2}\beta_2(t) - \frac{2\pi}{L+L_1}\omega(t)\alpha_2(t) \\
&\quad - \frac{\Gamma_1}{4\pi}(1-\cos 2\gamma) \\
\dot{\alpha}_3(t) &= -a\frac{9\pi^2}{(L+L_1)^2}\alpha_3(t) + \frac{3\pi}{L+L_1}\omega(t)\beta_3(t) \\
&\quad + \frac{\sin 3\gamma}{6\pi}\left[\Gamma_{\text{nom}} + K_{p\omega}(\omega_{\text{ref}}-\omega) + K_{dv}\dot{\omega}\right] \\
\dot{\beta}_3(t) &= -a\frac{9\pi^2}{(L+L_1)^2}\beta_3(t) - \frac{3\pi}{L+L_1}\omega(t)\alpha_3(t) \\
&\quad + \frac{1+\cos 3\gamma}{6\pi}\left[\Gamma_{\text{nom}} + K_{pv}(\omega_{\text{ref}}-\omega) + K_{dv}\dot{\omega}\right]
\end{aligned} \tag{35}$$

In order to determine the gain of the proportional controller, $K_{p\omega}$, it is necessary to analyse the stability of the controlled model (35) by varying $K_{p\omega}$, or, which is the same, to analyse the eigenvalues of the jacobian matrix of the controlled system.

These eigenvalues, i.e. the poles of the linearised controlled system, depends on $K_{p\omega}$ so that it can be determined by imposing that all the eigenvalues have negative real parts. This must be done considering the constraint that if the gain of the controller is too high it may happen the undesired condition of a *forced* convergence on the banal solution (i.e. point *SP*3), which corresponds to the flow stop.

In order to ensure a satisfactory margin of stability to the controlled system it has been found to be sufficient to require to the real parts of the poles to be minor than −0.00025.

The capabilities of the simple proportional action on the velocity have been tested in simulation for a wide range of initial conditions, demonstrating for all cases the ability of the controller in *capturing* the system dynamics in the basin of attraction of the stationary solution of the controlled system.

In the following plots, and unless differently stated, a horizontal dashed line will be used to indicate either the stationary value or the nominal value, depending on whether the plot reports one of the system variables or the control input. Analogously, a vertical dashed line will be used to indicate the instant at which the controller is activated.

Fig. 8 reports the results of the simulation performed for the operating condition with heat power in input $P = 1800$ W, calculated proportional gain $K_{p\omega} = -20.38$ and without derivative action ($K_{d\omega} = 0$). The left plot reports the evolution of the feedback variable, which exactly converges on the desired calculated stationary value, $\omega_{\text{ref}} = 0.0537$ m/s. The central plot reports the behaviour of the inlet–outlet temperature difference at the heating section whereas the right plot reports the control variable, the heat power P, whose oscillations with respect to the nominal value naturally vanishes, as well as $K_p(\omega_{\text{rif}} - \omega)$, once that system has been stabilised.

It is only mentioned here that, in consideration of the chaotic nature of the system, it has been also tested the behaviour of the system turning the controller off after that the stationary solution has been reached. Simulations of the model have shown that unstable chaotic oscillations occur again after a transient; their onset occurs after about 500 s from the time at which the controller is turned off.

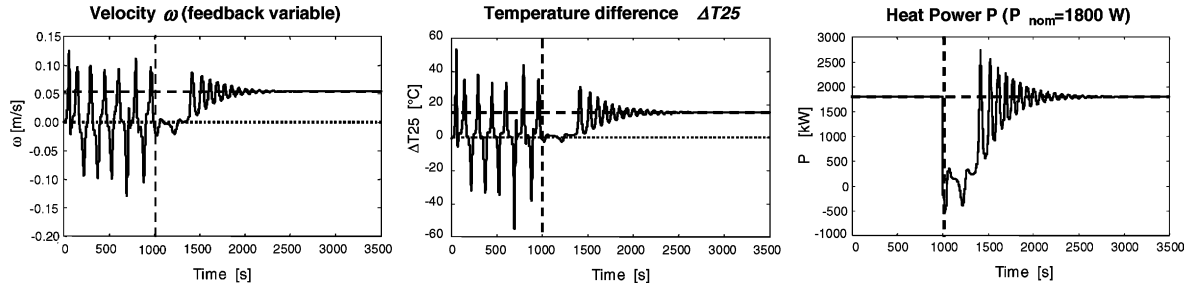

Fig. 8. Simulation of the proportional controller on the velocity for $P_{\text{nom}} = 1800$ W, $\omega_{\text{ref}} = 0.0537$ m/s, $K_{p\omega} = -20.38$: feedback variable ω (left plot), temperature difference $\Delta T25$ (central plot), control input P (right plot).

For the sake of comparability with the experimental data and of real application of the controller, a further modification to the emulator has been considered. In fact, the heat power, commanded from the control board, cannot vary unrestrained but must be bounded between a maximum, depending on the application, and a minimum, which can be hardly chosen below zero, as this would mean to operate the heating section as a cooling section. Various simulation have been performed with the emulator limiting the heat power within the range from 0 to 6000 W, with the upper limit corresponding to the maximum heat power that the experimental system is able to supply. Simulations performed in this way have revealed that the controller is always able to damp the oscillations and to drive the system to the desired target, though, as expected, this occurs in a wider transitory.

Considering the addition of the derivative term, simulations have allowed to observe, as expected theoretically, that it damps and shortens the transitory response of the controlled system.

The gain $K_{d\omega}$ has been determined maintaining the $K_{p\omega}$ previously calculated and proceeding by trials, trying to optimise the emulator response.

It has been found that the PD controller is effective for negative values of $K_{d\omega}$, ranging between $K_{d\omega} = -5$ and $K_{d\omega} = -100$. Moreover, the higher is the absolute value of the derivative gain, the stronger the oscillations are damped; for absolute value of $K_{d\omega}$ greater than 50, no further effective improvement of the performance occurs, whereas for $K_{d\omega}$ greater than 100 the simulated velocity settles down on the solution $SP3$.

Fig. 9 reports the time series of the feedback variable, ω, that has been obtained simulating the dynamics of the controlled system for a nominal heat power $P = 1800$ W, considering the same reference velocity ω_{ref} and proportional gain $K_{p\omega}$ previously considered. The left and right plots refer to the simulation performed for derivative gain $K_{d\omega} = -10$ and $K_{d\omega} = -50$ respectively. It can be noticed that the derivative term is beneficial as it allows a sensible reduction of the time required to the controller to drive the system to the stable solution: for example, for $K_{d\omega} = -10$ this time is about half of that required by the simple proportional controller. On the other hand, the reduction of the amplitude of the oscillations is not very relevant, though it occurs. The greater value for this gain allows to further reduce the controller time response and damp the oscillations, in particular avoiding flow reversal. Resuming, the controller has been demonstrated to be able to drive the system to the desired stationary value.

4.2. Proportional and proportional-derivative control on $\Delta T25$

Known applications of experimental control of natural circulation loops with toroidal geometry have considered the temperature difference between two sections of the loop as the feedback variable (see among the other [9,10,18,19]). A common choice is the temperature difference on the horizontal diameter, which in that configuration corresponds both to the inlet–outlet temperature difference at the heat exchanging sections and to one of the variable describing the mathematical model. This consideration has lead to choose also for the rectangular loop the inlet–outlet temperature difference at the heater, which has been called $\Delta T25$ in accordance to the first part of this study. This temperature difference has been calculated considering the abscissas $x_2 = 0.15$ m and $x_5 = (2L + L_1 - 0.15)$ m, which correspond to the measuring points of temperature $T2$ and $T5$ respectively, and applying Eq. (33) for the conversion from the model variable to the local temperature at the generic abscissa.

From a practical point of view this choice is preferable with respect to the velocity, as measuring the temperature is indeed easier, less expensive and more reliable than the flow rate.

The stationary temperature difference to be set as reference for the controller can be evaluated referring in Eq. (33) to the stationary values α_{101}, β_{101}, α_{201}, β_{201}, α_{301}, β_{301} (where the generic subscript $i01$ refers to the coefficient of the ith mode for the stationary point $SP1$).

Once that $\Delta T25_{\mathrm{ref}}$ has been defined the simple proportional-derivative control strategy produces the input:

$$\Gamma = \Gamma_{\mathrm{nom}} + K_{p\Delta T}(\Delta T25_{\mathrm{ref}} - \Delta T25) + K_{d\Delta T}\Delta\dot{T}25 \qquad (36)$$

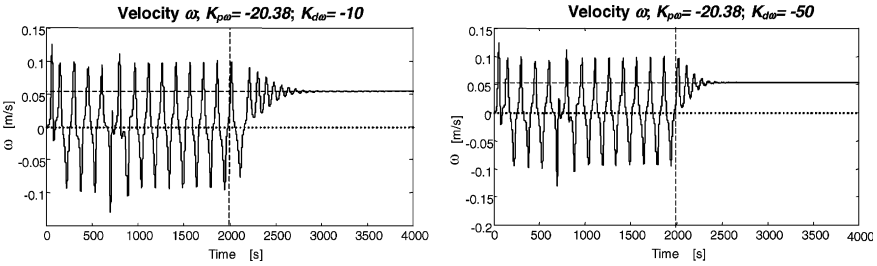

Fig. 9. Simulation of the PD controller on the velocity for $P_{\mathrm{nom}} = 1800$ W, $\omega_{\mathrm{rif}} = 0.0537$ m/s, $K_{p\omega} = -20.38$ and $K_{d\omega} = -10$ (left plot), $K_{d\omega} = -50$ (right plot).

and the ODE model for the controlled system becomes

$$\begin{aligned}
\dot{\omega}(t) &= -\frac{1}{r}b\left(\frac{v}{2r}\right)^{d}\omega^{2-d} + \frac{2g\beta}{\pi}\left[\alpha_1(t)\sin\gamma - \beta_1(t)\right.\\
&\quad\left.\times(1-\cos\gamma) + \alpha_3(t)\frac{1}{3}\sin 3\gamma - \beta_3(t)\frac{1}{3}(1-\cos 3\gamma)\right]\\
\dot{\alpha}_1(t) &= -a\frac{\pi^2}{(L+L_1)^2}\alpha_1(t) + \frac{\pi}{L+L_1}\omega(t)\beta_1(t) + \frac{\sin\gamma}{2\pi}\\
&\quad\times\left[\Gamma_{\text{nom}} + K_{p\Delta T}(\Delta T25_{\text{ref}} - \Delta T25) + K_{d\Delta T}\Delta\dot{T}25\right]\\
\dot{\beta}_1(t) &= -a\frac{\pi^2}{(L+L_1)^2}\beta_1(t) - \frac{\pi}{L+L_1}\omega(t)\alpha_1(t) + \frac{(1+\cos\gamma)}{2\pi}\\
&\quad\times\left[\Gamma_{\text{nom}} + K_{p\Delta T}(\Delta T25_{\text{ref}} - \Delta T25) + K_{d\Delta T}\Delta\dot{T}25\right]\\
\dot{\alpha}_2(t) &= -a\frac{4\pi^2}{(L+L_1)^2}\alpha_2(t) + \frac{2\pi}{L+L_1}\omega(t)\beta_2(t) + \frac{\Gamma_1}{4\pi}\sin 2\gamma\\
\dot{\beta}_2(t) &= -a\frac{4\pi^2}{(L+L_1)^2}\beta_2(t) - \frac{2\pi}{L+L_1}\omega(t)\alpha_2(t) - \frac{\Gamma_1}{4\pi}\\
&\quad\times(1-\cos 2\gamma)\\
\dot{\alpha}_3(t) &= -a\frac{9\pi^2}{(L+L_1)^2}\alpha_3(t) + \frac{3\pi}{L+L_1}\omega(t)\beta_3(t) + \frac{\sin 3\gamma}{6\pi}\\
&\quad\times\left[\Gamma_{\text{nom}} + K_{p\Delta T}(\Delta T25_{\text{ref}} - \Delta T25) + K_{d\Delta T}\Delta\dot{T}25\right]\\
\dot{\beta}_3(t) &= -a\frac{9\pi^2}{(L+L_1)^2}\beta_3(t) - \frac{3\pi}{L+L_1}\omega(t)\alpha_3(t) + \frac{1+\cos 3\gamma}{6\pi}\\
&\quad\times\left[\Gamma_{\text{nom}} + K_{p\Delta T}(\Delta T25_{\text{ref}} - \Delta T25) + K_{d\Delta T}\Delta\dot{T}25\right]
\end{aligned} \tag{37}$$

From this point on, the strategy that has been followed is identical to that for the velocity. In particular, the proportional gain has been determined imposing the stability of the linearised system, finding the $K_{p\Delta T}$ ensuring that the real parts of the linearised system is minor than a specified value (set equal to −0.001). Values of $K_{p\Delta T}$ for which this happens have been proved to exist in all the range of nominal operating conditions considered.

For the case of the heat power $P_{\text{nom}} = 1800$ W, for which $\Delta T25_{\text{ref}} = 15$ °C, it has been found $K_{p\Delta T} = 50$. This value has been tested in simulation, showing that the system dynamics in this case is not stabilised on the desired stationary solution but that the controller drive the system to the no-flow condition, i.e. point $SP3$. Various other values of $K_{p\Delta T}$ have been therefore tested on the emulator. This has lead to find that proportional gain $K_{p\Delta T} = -0.07$ is able to stabilise the simulated dynamics on the desired stationary solution $\Delta T25_{\text{ref}}$. Correspondingly, also the simulated velocity has been proved to reach its stationary value at $P_{\text{nom}} = 1800$ W.

Fig. 10 shows the simulated results of the simple proportional strategy ($K_{d\Delta T} = 0$) for the mentioned values of P_{nom} and $\Delta T25_{\text{rif}}$ and for $K_{p\Delta T} = -0.07$. The controller has been turned on in presence of well-developed unstable oscillations. Also in this case it has been chosen to describe directly the simulations obtained taking into account the possibility to vary the heat power P only once out of 5 s. Moreover, the heat power P has been bounded in the range between 0 and 6000 W.

The only difference with respect to what has been previously described for the controller on the velocity is the introduction of a white noise acting on the velocity (obtained with a new block in the emulator), with a maximum amplitude of the 2% of the stationary value of this variable. The choice of the velocity has been made because this is the only real variable appearing in the ODE model and this is the most feasible way to represent the influence of noise on the whole system.

The analysis of the plots evidences that simulations of the controller converge on the desired target; the amplitude of the oscillations are in the overall comparable with those obtained with the controller on the velocity, pointing out that both temperature difference $\Delta T25$ and velocity ω can be theoretically chosen.

Notice that reported simulations demonstrate that the choice of $K_{p\Delta T} = -0.07$, though derived by means of the emulator and not from the linearised model, allows the control on $\Delta T25$ to perform as satisfactorily as the control on velocity. This result has been confirmed in the experiments, as reported in the next section.

Fig. 11 reports the results of the simulations performed for a derivative gain $K_{d\Delta T} = -2$, and for the

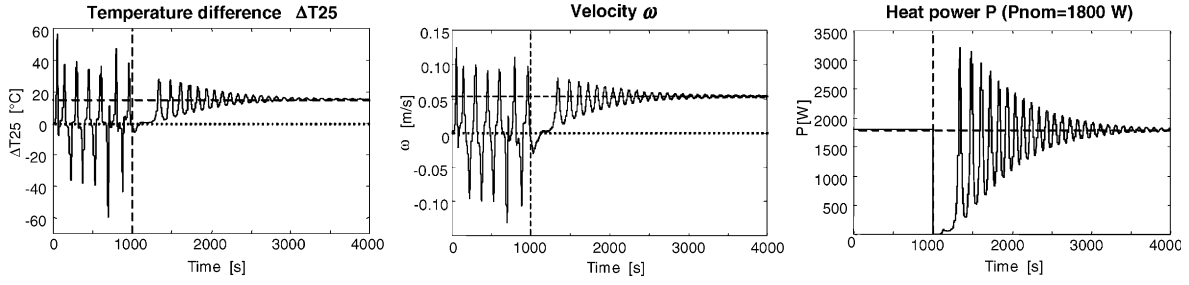

Fig. 10. Simulation of the proportional control on temperature difference $\Delta T25$ for $P_{\text{nom}} = 1800$ W, $\Delta T25_{\text{ref}} = 15$ °C, $K_{p\Delta T} = -0.07$: feedback variable $\Delta T25$ (left plot), velocity ω (central plot), control input P (right plot).

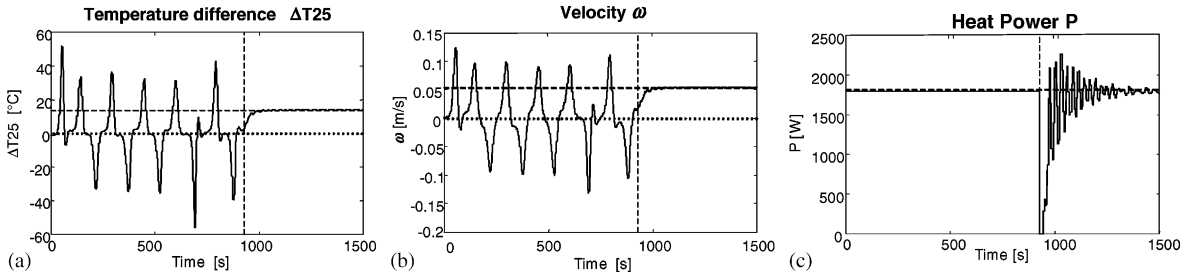

Fig. 11. Simulation of the PD controller on temperature difference $\Delta T25$ for $P_{nom} = 1800$ W, $\Delta T25_{ref} = 15$ °C, $K_{p\Delta T} = -0.07$, $K_{d\Delta T} = 2$: (a) $\Delta T25$, (b) P, (c) ω.

other conditions considered for the simple proportional strategy. The only difference between the two tests is the time at which the controller has been activated. This choice has been made because the activation of the PD controller after 1000 s (and for the same initial conditions) has shown a very fast convergence on the stationary solutions. This happens because the starting of the controller at initial state very close to solution $SP3$ causes the capturing of the system dynamics, damping to zero the heat power supply; this brief initial transient produces the drastic damping of the oscillations, which is then followed by a sort of unrealistic overdamped convergence to the desired stationary behaviour.

The analysis of the plots evidences that the derivative action seems to determine, at least in simulation, a drastic improvement of the convergence of the system. The transient of the controlled system is, in fact, shorter and, above all, the oscillations of the system variables are much lower.

Reported results have been all referred, for brevity, to a nominal heat power $P_{nom} = 1800$ W. Nonetheless, a wide set of heat power values, covering the entire range of interest, have been examined and the corresponding control parameters have been calculated. The procedure that has been adopted perfectly corresponds to that described so far; also, the results of the simulations are consistent with those previously reported.

Table 4 summarises the gain of the controllers that have ensured the desired performance for the various controllers. In all reported cases the gains of the proportional control either on velocity ω or on temperature difference $\Delta T25$ have not been altered during the design of the proportional-derivative controller.

5. Experimental control

This section is devoted to draw a schematic picture of the results that have been obtained applying the control strategies previously discussed to the experimental apparatus described in the second section. For each controller reported in the previous section, various experimental tests have been performed in order to adjust the reference values and the controller gains to be used during the experiments, starting from those determined on the base of the mathematical model and of its simulations. A general criterion adopted has been to search for a good settling time without a large overshoot, in order to achieve suitable performances of the controller. For brevity, among those experimented, only the results corresponding to the most satisfactory performances of the various controllers have been reported.

Preliminary tests have been performed for various nominal heat power, P_{nom}, activating the simple proportional controller, either on the velocity or on temperature difference $\Delta T25$, with the reference value and gains defined on an analytical base from the quiet condition. This has allowed to experimentally determine case by case the real stationary values of the model variables on which the dynamics of the real controlled system converge; hence, the controller gains have been adjusted in order to account for the mismatch between

Table 4
Summary of the calculations of the P and PD controllers on ω and on $\Delta T25$ for various nominal heat power P_{nom}

P [W]	ω_{ref} [m/s]	$K_{p\omega}$	$K_{d\omega}$	$\Delta T25_{ref}$ [°C]	$K_{p\Delta T}$	$K_{d\Delta T}$
1000	0.0407	−15.06	−15	11.17	−0.0500	−0.5
1200	0.0444	−16.57	−15	12.28	−0.0554	−0.5
1400	0.0477	−17.96	−15	13.32	−0.0595	−0.7
1600	0.0512	−18.98	−10	14.19	−0.0650	−0.7
2000	0.0560	−21.72	−20	16.22	−0.0800	−0.8
2200	0.0582	−23.00	−15	17.18	−0.1000	−1.0
2400	0.0602	−24.24	−15	18.10	−0.1000	−1.0

the model and the experimental system. Notice that, for each test the desired stationary behaviour has been satisfactorily reached. This has been verified also for cases in which the controller have been turned on from a well-developed unstable dynamics; the only drawback that has been revealed in these tests is that the error on the reference stationary value causes a slight growth of the controller settling times.

The overall good performances of the analytical control demonstrate the validity of the model and the robustness of the proposed control strategies to uncertainty on the model parameters. This is indeed an important result in consideration of the chaotic nature of the free dynamics of the system.

For the sake of comparability with the results of the simulations reported in the previous section, the experimental test with nominal heat power $P_{\mathrm{nom}} = 1800$ W will be reported. For this test the velocity reference value has been corrected, as previously described, passing from the theoretical value $\omega_{\mathrm{ref}} = 0.0537$ m/s to the experimental value $\omega_{\mathrm{ref}} = 0.0628$ m/s. Correspondingly, the stationary value of $\Delta T25$ has been decreased from the theoretical $\Delta T25_{\mathrm{ref}} = 15$ °C to the experimental $\Delta T25_{\mathrm{ref}} = 11$ °C. The proportional gain of the controller has been settled at $K_{p\omega} = -20$, which very slightly differs from the theoretical $K_{p\omega} = -20.38$.

The left column of Fig. 12 reports the experimental time series of the controlled system under the previous choices and with feedback on the velocity. The upper plot reports only the experimental time series of the feedback variable with the control on, so that the comparison with the third plot, reporting the control input P, can be easily done. The second plot reports both the controlled and the uncontrolled temperature difference $\Delta T25$, in order to allow to esteem the ability of the controller in suppressing unstable chaotic dynamics.

The analysis of the reported time series evidences that the experimental controller performs satisfactorily, driving the system dynamics to the desired stationary solutions in a reasonably short time. Nonetheless, it can be observed that the activation of the controller has not corresponded to the complete disappearance of flow reversals (at least one has still occurred). Moreover, even when the desired steady state has been reached, the control input continues to oscillate, which means that the *cost of control* is in this case higher. The reason of this behaviour is the relevant amount of noise that affects the measure of the velocity, which is a main drawback in the choice of this one as the feedback variable. Notice that the results herein reported (with a cut-off filter at 0.1 Hz on the velocity) are the best obtainable: this is an intrinsic constraint of the magnetic

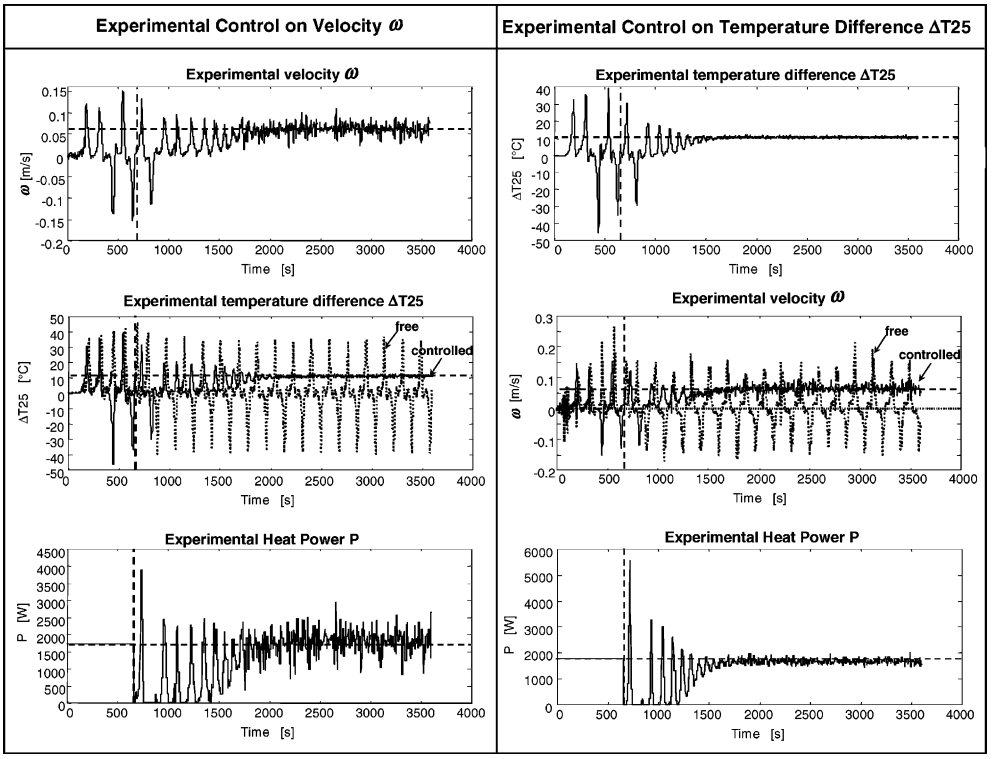

Fig. 12. Experimental proportional control on the velocity (left column) and on the temperature difference for $P_{\mathrm{nom}} = 1800$ W: feedback variable (first row), independent variable with and without control (second row), control input P (third row).

flow meter adopted for the measure of the velocity, which is affected (in the whole range of frequencies of interest) by the presence of impurity and small water vapour bubbles transported by the flow. Nonetheless, this is the only sensor which can be used in the present application, as other kind of flow meter, non-magnetic, interact in some way with the flow dynamics (usually with a concentrated loss). Fortunately, it has been verified that when the system reaches the desired stationary behaviour it is possible to eliminate the controller indefinitely. In fact, unless a sudden perturbation of the heat power of relevant amplitude (of about 350 W) is applied, the experimental system dynamics remains stationary. The last consideration represents an experimental evidence of the existence of a basin of attraction of the stationary solution with non-null measure that can be considered the result of various damping inertial term, acting on the flow dynamics in a way that is not contemplated by the model. In practice, once that the system dynamics has been stabilised and a well-developed turbulent flow is established, the new damping terms acting on the process are not those considered in the model during the calculation (as reported in Table 3 for heat power greater than 900 W) but are greater. This means that they are able to damp external perturbation more strongly then those considered for the free dynamics.

Considering as feedback variable the temperature difference $\Delta T25$, the approach followed to determine the optimal parameters of the controller is the same described for the velocity. In particular, though it had been considered obvious, it has been nonetheless verified the correspondence of the experimental stationary conditions on which the controlled system *naturally* converges, i.e. when the tests are started directly with the control on, with those determined with the control on the velocity.

For example, considering, as in previous cases, the test with $P_{\mathrm{nom}} = 1800$ W, the reference value for the feedback variable has been found again to be $\Delta T25_{\mathrm{ref}} = 11$ °C, corresponding to $\omega_{\mathrm{ref}} = 0.63$ m/s and leading to a "corrected" proportional gain $K_{p\Delta T} = -0.12$. The mismatch of 4 °C between the stationary predicted and experimental value is due to the heat lost from the various parts of the experimental loop (which is not modelled at all). These losses have the global effect to decrease the *thermal level* of the system, leading to lower stationary states. This effect could be modelled, but this is out of the aims of this study, by subtracting a constant term (representing the mean value of the heat losses over the whole loop) to the function $h(x)$ used in this study to describe the boundary heating conditions.

The right column of Fig. 12 reports the experimental time series of the controlled system with $\Delta T25$ as feedback variable. The first row reports only the feedback variable $\Delta T25$, the second plot reports the velocity ω both under the controlled and the free condition, in order to allow to judge qualitatively the capability of the controller and the third plot reports the heat power P, i.e. the control input.

Though also in this case the controller is not able to avoid from the very beginning the flow reversal, its performances are not only satisfactory on the overall, but are sensibly better than those obtained with the feedback on the velocity. In fact, oscillation amplitude as well as the controller settling time are sensibly reduced and, even more important in practice, the control input oscillations around its equilibrium nominal value are drastically lower, which implies a reduction of the *cost of control*. This was an expected result, as the measurement of the temperature by means of thermocouples is more reliable and less sensitive to noise than the measurement of the velocity by means of the magnetic flow meter equipping the experimental apparatus.

In order to give a synthetic presentation of the performances of the proportional controller in the whole range of nominal heat power of interest, Figs. 13 and 14 report the results of the proportional strategy on ω and on $\Delta T25$ respectively, for nominal heat power $P_{\mathrm{nom}} = 1400$ W (left column) and $P_{\mathrm{nom}} = 2200$ W (right column). It must be reminded that, as it has been described in the section devoted to the validation of the model, the free dynamics manifested by the system for these two values of P_{nom} is considerably different. In particular, for $P_{\mathrm{nom}} = 2200$ W the system behaviour only slightly differs from that at $P_{\mathrm{nom}} = 1800$ W (i.e. just in term of stationary values and of maximum excursions of the system variables), whereas the behaviour at $P_{\mathrm{nom}} = 1400$ W is relevantly different, as the system oscillates only around one of the two symmetric stationary points $SP1$ and $SP2$. In terms of phase space representation, this corresponds to an attractor with one single lobe, which is morphologically quite different from the attractor with two lobes obtainable for higher values of P_{nom}.

The results reported in both figures show that the proportional control strategy on both variables is effective in stabilising the two kind of system dynamics that the system may manifest; this means that it can be usefully applied over the entire operating range of the experimental system. Note also that for all the reported values of the nominal heat power, the use as feedback variable of the temperature difference instead of the velocity allows higher performances. Finally, it has been also observed that the use of a proportional control does not sensibly amplify disturbances, which are anyway very low. The only drawback manifested for the control on temperature difference $\Delta T25$ at $P_{\mathrm{nom}} = 2200$ W consists in the mismatch existing between the value of the heat power at steady state and the desired nominal

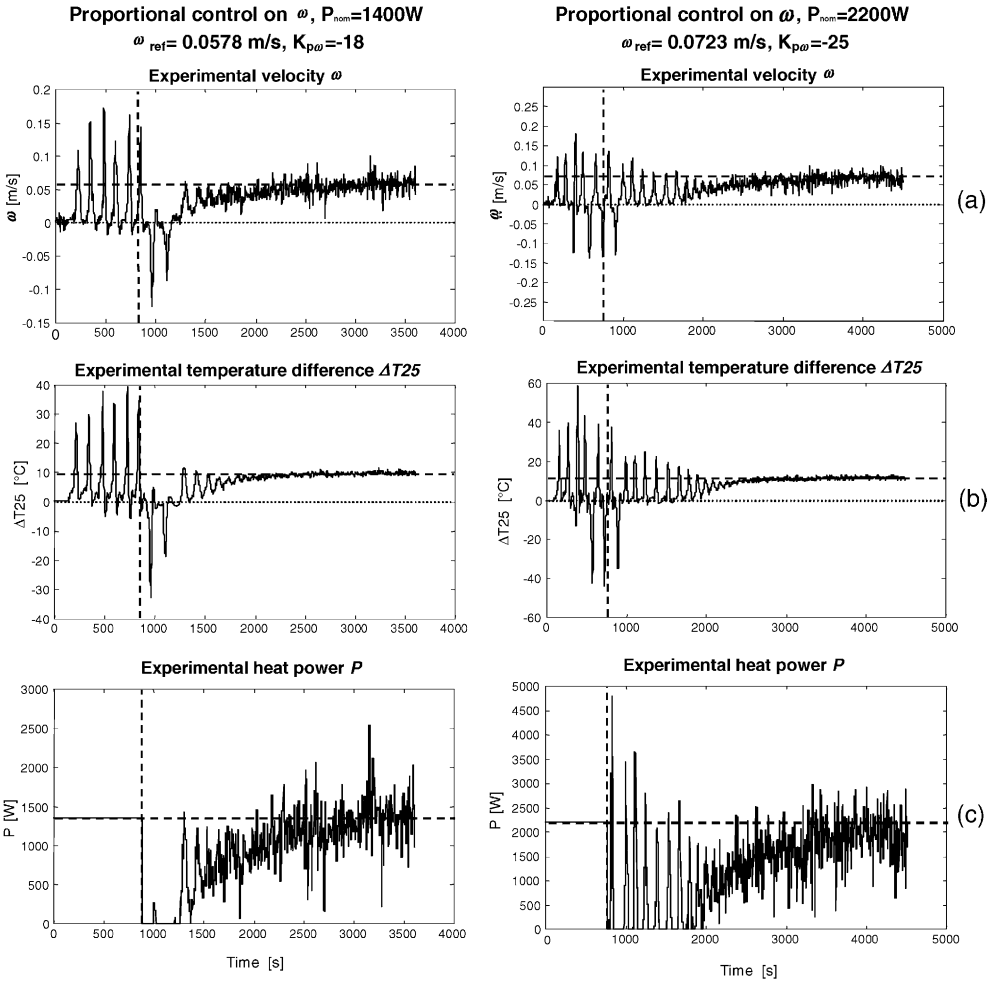

Fig. 13. Experimental proportional control on the velocity for $P_{\text{nom}} = 1400$ W (left column) and $P_{\text{nom}} = 2200$ W (right column): (a) feedback variable ω, (b) temperature difference $\Delta T25$, (c) control input P.

value. Further experimental tests, with opportune adjustments of the proportional gain of the controller, would allow to eliminate this mismatch but is beyond the scope of this paper.

Table 5 reassumes a schematic of the reference stationary values and of the corresponding gains experimentally determined at various nominal heat power values for the proportional controller with feedback respectively on the velocity and on temperature difference $\Delta T25$.

Finally, the experimental tests for the PD control strategy have been concentrated only on the PD control on temperature difference $\Delta T25$, due to the better performances ensured by the simple proportional control on this variable with respect to that on velocity. Fig. 15 summarises the experimental results obtained for the heat power $P_{\text{nom}} = 1800$ W, for the same proportional gain $K_{p\Delta T}$ used for the simple proportional control (which is also reported in the figure) and for three different values of the derivative gain $K_{d\Delta T}$: −0.25, −0.5 and −0.75. For the sake of comparability, though the system is chaotic it has been chosen to activate the controller after 630 s for all the tests. Notwithstanding the differences characterising the initial part of the various tests, this has allowed to activate the controller for a similar initial state of the system.

The analysis of the plots evidences that the addition of the derivative action has the desired effect: the oscillations are in fact increasingly damped for growing values of the $K_{d\Delta T}$. Nonetheless, it can be noticed that for $K_{d\Delta T} = -0.75$ the system converges more slowly to the stationary solution; moreover, this value of the derivative gain causes the worsening of the control input once that the regime has been reached, as a consequence of the amplified effect of noise on the derivative of the feedback variable. In practice, the derivative gain $K_{d\Delta T} = -0.5$ ensures in the overall the best performances as it presents the fastest convergence, low amplitudes of

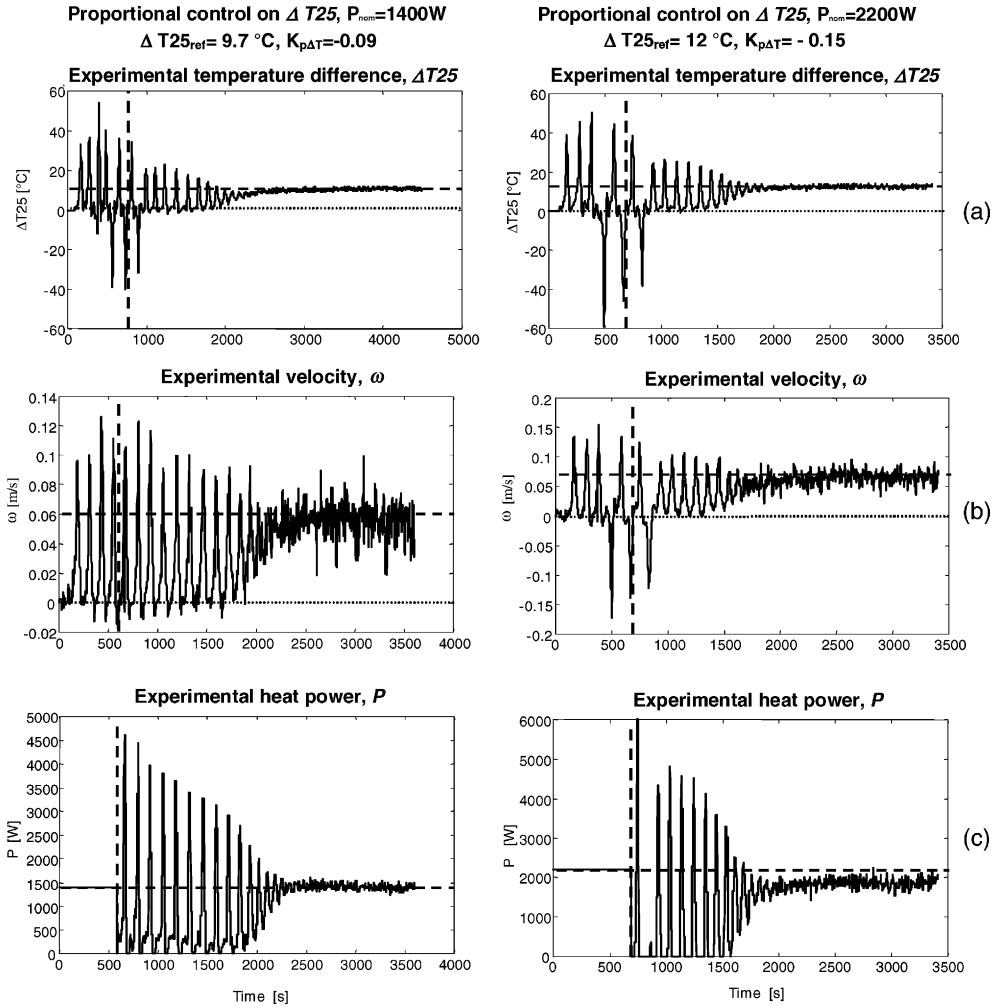

Fig. 14. Experimental proportional control on $\Delta T25$ for $P_{\text{nom}} = 1400$ W (left column) and $P_{\text{nom}} = 2200$ W (right column): (a) feedback variable $\Delta T25$, (b) velocity ω, (c) control input P.

Table 5
Summary of the calculations of the P and PD controllers on ω and on $\Delta T25$ for various nominal heat power P_{nom}

P_{nom} [W]	ω_{ref} [m/s]	$K_{p\omega}$	$\Delta T_{25\text{ref}}$ [°C]	$K_{p\Delta T}$
1000	0.0477	−16	8.30	−0.06
1200	0.0538	−17	9.08	−0.08
1400	0.0578	−18	9.69	−0.09
1600	0.0601	−19	10.04	−0.11
1800	0.0628	−20	11.00	−0.12
2000	0.0680	−23	11.50	−0.14
2200	0.0723	−25	12.00	−0.15

the oscillations and, at regime, sufficiently low influence of noise on the control input.

In practice, though the derivative action has allowed to slightly decrease the settling time, it has not introduced significant improvements. Similar results have been obtained for the whole set of nominal equilibrium points considered.

6. Conclusions

In this study a finite order model and a controller for rectangular natural circulation loops have been theoretically defined and experimentally validated. The model has been obtained by reducing an infinite set of equations, derived by the Fourier series expansion of the momentum and energy equations, to a truncated finite set of seven equations approximating the system dynamics to the first three modes. Comparisons of experimental and simulated time series in the time domain and in phase space have confirmed the reliability of the

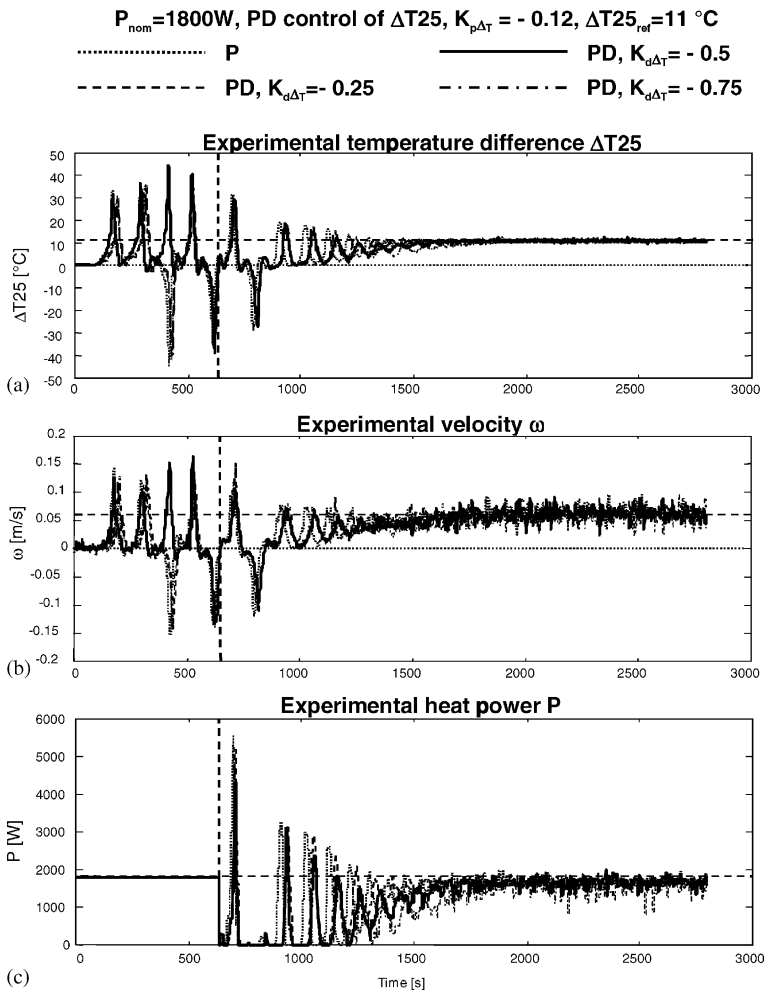

Fig. 15. Experimental PD control on $\Delta T25$, $P_{\text{nom}} = 1800$ W, $\Delta T25_{\text{ref}} = 11$ °C, $K_{p\Delta T} = -0.12$ and various gain: (a) feedback variable $\Delta T25$, (b) velocity ω, (c) control input P.

model, which correctly reproduces the complex dynamics displayed by real systems.

Two distinct feedback variables have been considered for the design of the model-based controller: the flow velocity and the inlet–outlet temperature difference at the heating section. The first variable has never been used in similar experimental implementation whereas the temperature difference has represented the common choice. Theoretical and experimental applications of the proportional control, on both variables, have allowed to stabilise the system dynamics, though a slight mismatch between the experimental and simulated results still exists. Nonetheless, reported results represent a step ahead with respect to previous studies, for which the passage from theory to experiments has required not only strong modification of the parameters of the controller but even the use of a different control law.

Acknowledgements

The authors wish to acknowledge the very useful help of G. Muscato and M.G. Xibilia, whose contribution in the design of the experimental controller has been fundamental.

References

[1] P.K. Vijayan, A.K. Nayak, D.S. Pilkhwal, D. Saha, V. Venkat Raj, Effect of loop diameter on the stability of single-phase natural circulation in rectangular loops, in: Proc. 5th Int. Topical Meet. on Reactor Thermal Hydraulics (NURETH-5), vol. 1, Salt Lake City, 1992, pp. 261–267.

[2] J. Miettinen, T. Kervinen, H. Tomisto, H. Kantee, Oscillations of single-phase natural circulation during

overcooling transient, in: Proc. ANS Topical Meet., vol. 1, Atlanta, 1987, pp. 20–29.
[3] R. Greif, Y. Zvirin, A. Mertol, The transient and stability behavior of a natural convention loop, Trans. ASME 101 (1979) 684–688.
[4] D.B. Kreitlow, G.M. Reistad, C.R. Miles, G.G. Culver, Thermosyphon models for downhole heat exchanger applications in shallow geothermal systems, ASME J. Heat Transfer 100 (1978) 713–719.
[5] Y. Zvirin, A. Shitzer, A. Bartal-Bornstein, On the stability of the natural circulation solar heater, in: Proc. 6th Int. Heat Transfer Conf., vol. 20, Toronto, 1978, pp. 997–999.
[6] Y. Zvirin, A review of N.C. loops in PWR and other systems, Nucl. Eng. Des. 67 (1981) 203–225.
[7] D. Japikse, Advances in thermosyphon technology, in: T.F. Irvine, J.P. Harnett (Eds.), Advances in Heat Transfer, vol. 9, 1973, p. 111.
[8] G. Cammarata, A. Fichera, M. Froghieri, M. Misale, M.G. Xibilia, A new modelling methodology of natural circulation loop for stability analysis, in: Proc. Eurotherm Semin. 63, Genova, 1999, pp.151–159.
[9] Y.-Z. Wang, J. Singer, H.H. Bau, Controlling chaos in a thermal convection loop, J. Fluid Mech. 237 (1992) 479–498.
[10] J. Singer, Y.-Z. Wang, H.H. Bau, Controlling a chaotic system, Phys. Rev. Lett. 66 (9) (1991) 1123–1125.
[11] M. Sen, E. Ramos, C. Trevino, O. Salazar, A one-dimensional model of a thermosyphon with known wall temperature, Int. J. Heat Fluid Flow 8 (3) (1987) 171–181.
[12] M. Sen, E. Ramos, C. Trevino, The toroidal thermosyphon with known heat flux, Int. J. Heat Mass Transfer 28 (1) (1985) 219–233.
[13] M. Sen, E. Ramos, C. Trevino, O. Salazar, The effect of axial conduction on a thermosyphon with prescribed heat flux, Eur. J. Mech., B-Fluids 8 (1) (1989) 57–72.
[14] H.H. Bau, K.E. Torrance, Transient and steady behavior of an open, symmetrically-heated, free convection loop, Int. J. Heat Mass Transfer 24 (1981) 597–609.
[15] M. Gorman, P.J. Widman, K.A. Robbins, Nonlinear dynamics of a convection loop: a quantitative comparison of experiment with theory, Physica D 19 (1986) 255–267.
[16] P.J. Widman, M. Gorman, K.A. Robbins, Nonlinear dynamics of a convection loop II: chaos in laminar and turbulent flows, Physica D 36 (1989) 255–267.
[17] E.N. Lorenz, Deterministic nonperiodic flow, J. Atmos. Sci. 20 (1963) 131–141.
[18] J. Singer, H.H. Bau, Active control of convection, Phys. Fluids A 3 (12) (1991) 2859–2865.
[19] Y.-Z. Wang, J. Singer, H.H. Bau, Rendering a subcritical hopf bifurcation supercritical, J. Fluid Mech. 317 (1992) 479–498.
[20] H.O. Wang, E.H. Abed, Bifurcation control of a chaotic system, Automatica 31 (9) (1995) 1213–1226.
[21] A. Rodriguez-Bernal, E. Van Vleck, Diffusion induced chaos in a closed loop thermosyphon, SIAM J. Appl. Math. 58 (4) (1998) 1072–1093.
[22] P.K. Yuen, H.H. Bau, Controlling chaotic convection using neural networks—theory and experiments, Neural Networks 11 (1998) 557–569.
[23] P.K. Yuen, H.H. Bau, Optimal and adaptive control of chaotic convection—theory and experiments, Phys. Fluids 11 (6) (1999) 1435–1448.
[24] J.A. Yorke, E.D. Yorke, J. Mallet-Paret, Lorenz-like chaos in a partial differential equation for a heated fluid loop, Physica D 24 (1987) 279–291.
[25] S.N. Rasband, Chaotic Dynamics of Nonlinear Systems, J. Wiley & Sons, New York, 1990.
[26] J.M.T. Thompson, H.B. Stewart, Nonlinear Dynamics and Chaos, J. Wiley & Sons, New York, 1986.